Driven maps and the emergence of ordered collective behavior in globally coupled maps

A. Parravano and M. G. Cosenza
Centro de Astrofísica Teórica, Facultad de Ciencias, Universidad de Los Andes, Apartado Postal 26 La Hechicera, Mérida 5251, Venezuela

(Received 5 August 1997; revised manuscript received 23 February 1998)

A method to predict the emergence of different kinds of ordered collective behaviors in systems of globally coupled chaotic maps is proposed. The method is based on the analogy between globally coupled maps and a map subjected to an external drive. A vector field which results from this analogy appears to govern the transient evolution of the globally coupled system. General forms of global couplings are considered. Several applications are given. [S1063-651X(98)05507-X]

PACS number(s): 05.45.+b, 02.50.−r

I. INTRODUCTION

Coupled map lattices constitute useful models for the study of spatiotemporal processes in a variety of contexts [1]. There has been recent interest in the investigation of the emergence of ordered collective behaviors (OCB's) in systems of interacting chaotic elements by using coupled map lattices [2–5]. Such cooperative phenomena have been considered relevant in many physical and biological situations [6–9]. In particular, globally coupled maps (GCM's) [10] can exhibit OCB's such as (a) formation of clusters, i.e., differentiated subsets of synchronized elements within the network [11]; (b) nonstatistical properties in the fluctuations of the mean field of the ensemble [11,12]; (c) global quasiperiodic motion [13,14]; and different collective phases depending on the parameters of the system [13].

Much effort has been dedicated to establishing the necessary conditions for the emergence of various types of OCB's, mostly involving direct numerical simulations on the whole globally coupled system. However, this direct procedure gives little information about the mechanism for the emergence of OCB's. In this paper, we propose an alternative method which allows us to gain insight into the conditions for the emergence of specified types of collective behavior.

The procedure is suggested by the analogy between a globally coupled map system

$$x_{t+1}^n=(1-\epsilon)f(x_t^n)+\epsilon H(x_t^1,x_t^2,\ldots,x_t^N) \tag{1}$$

and an associated driven map

$$s_{t+1}=(1-\epsilon)f(s_t)+\epsilon L_t. \tag{2}$$

In Eq. (1), x_t^n $(n=1,\ldots,N)$ is the state of the nth element at discrete time t, N is the size of the system; ϵ is the coupling parameter, $f(x)$ describes the local dynamics, and $H(x_t^1,x_t^2,\ldots,x_t^N)$ is the global coupling function. A commonly used form for H is the mean field coupling [10,12,14]; however, the global coupling $H_t=H(x_t^1,x_t^2,\ldots,x_t^N)$ in Eq. (1) is assumed to be any function invariant to argument permutations. In Eq. (2), s_t is the state of the driven map at a discrete time t, $f(s_t)$ is the same local dynamics as in Eq. (1), and L_t is the driving term. In general, L_t may be any function of time.

After a transient time required to reach the OCB, the asymptotic collective behavior of the GCM system is characterized, in many cases, by a periodic or quasiperiodic time evolution of the mean state $\langle x\rangle_t$ and of the coupling function H_t. The elements of the system follow a behavior similar to H_t, and in general are segregated in clusters which tend to be out of phase [10]. Here we focus on the relationship between periodically driven maps and the emergence of periodic and quasiperiodic OCB's in GCM's.

In Sec. II, a relation between driven maps and GCM's is established. A method for predicting clustered OCB's in globally coupled maps is presented in Sec. III. Several applications of the method are shown in Sec. IV. Finally, a discussion of the possibilities and limitations of the method is given in Sec. V.

II. RELATION BETWEEN DRIVEN MAPS AND GCM'S

Note that the evolution of any element in the GCM is determined by the initial conditions of the whole system through H, while the evolution of the driven map is determined by its initial condition s_1 and L_t. The basic fact that allows one to establish a relationship between driven maps and GCM's is that in GCM systems all the elements are affected by the coupling in exactly the same way at all times, and therefore the behavior of the element x_t^n in the GCM is equivalent to the behavior of a single driven map [Eq. (2)], with $L_t=H_t$ and initial condition $s_1=x_1^n$.

Additionally, if a GCM [Eq. (1)] reaches an OCB, H_t displays in general an ordered asymptotic behavior. Therefore, the associated driven map [Eq. (2)] for these asymptotic ordered states of GCM's should contain a rather regular drive L_t. Conversely, the study of the dynamics of Eq. (2) for a given class of drives L_t can provide information about the possible existence of a similar class of OCB's in corresponding GCM's, without doing a direct simulation on the the latter system. In particular, periodic drives resulting in a periodic asymptotic state of s_t in Eq. (2) may be used to predict the emergence of a periodic or quasiperiodic OCB in a GCM [Eq. (1)].

In order to compare the dynamics of the GCM and the driven map, it is useful to introduce some notation for their asymptotic periodic regimes. For a GCM, described by Eq. (1), consider the case of an OCB consisting of K clusters

with period P. In this case, the asymptotic behavior of the system can be characterized by a $K\times P$ matrix

$$\boldsymbol{\chi}=\begin{pmatrix} \chi_1^1 & \cdots & \chi_1^K \\ & \ddots & \\ \vdots & \chi_i^k & \vdots \\ & \ddots & \\ \chi_P^1 & \cdots & \chi_P^K \end{pmatrix}, \tag{3}$$

where the kth column contains the temporal sequence of the P values adopted by the elements belonging to the kth cluster; and the ith row displays the state of all clusters at time i. The time step t has been replaced by the index i which runs from 1 to the periodicity P. Denoting by Φ_i $(i=1,2,\ldots,P)$ the asymptotic values adopted by the global coupling H_t, we have

$$\Phi_i = H(\underbrace{\chi_i^1,\ldots,\chi_i^1}_{N_1\,\text{times}},\ldots,\underbrace{\chi_i^k,\ldots,\chi_i^k}_{N_k\,\text{times}},\ldots,\underbrace{\chi_i^K,\ldots,\chi_i^K}_{N_K\,\text{times}}), \tag{4}$$

where N_k is the number of elements in the kth cluster and $\Sigma_k N_k = N$. Thus we may express the asymptotic temporal behavior of H_t by the vector $\vec{\Phi}=(\Phi_1,\ldots,\Phi_i,\ldots,\Phi_P)$.

On the other hand, for a driven map subjected to a periodic drive L_t with period P, a similar notation can be established. The long-term response of s_t depends on the initial condition s_1, and on the specific sequence of values adopted by L_t, which we will denote as the vector $\vec{L}=(L_1,\ldots,L_i,\ldots,L_P)$. The response $s_t(\vec{L},s_1)$ may be periodic on a region R of the P-dimensional space spanned by all possible vectors $\vec{L}$. For a given $\vec{L}\in R$, there are, usually, J different asymptotic periodic responses of s_t with period M, each one associated with a set of initial conditions $\{s_1\}_j$, where $j=1,2,\ldots,J$. It may happen that all the asymptotic responses do not have the same period, but are submultiples of the response with maximum periodicity. In this case, all the asymptotic periodic responses can be seen as having the same maximum periodicity M. If we denote by σ_i^j $(i=1,2,\ldots,M)$ the asymptotic periodic response of $s_t(\vec{L},s_1)$, that is, reached for $s_1\in\{s_1\}_j$, then all the possible asymptotic responses can be represented by the $J\times M$ matrix

$$\boldsymbol{\sigma}=\begin{pmatrix} \sigma_1^1 & \cdots & \sigma_1^J \\ & \ddots & \\ \vdots & \sigma_i^j & \vdots \\ & \ddots & \\ \sigma_M^1 & \cdots & \sigma_M^J \end{pmatrix}, \tag{5}$$

where the jth column contains the asymptotic periodic response of s_t for the initial states $s_1\in\{s_1\}_j$, and the ith row displays the state of all the possible asymptotic responses at time i. As before, the time step t has been replaced by the index i running from 1 to the periodicity M of the response. The region R may consist of various subregions R_M^J, where J different asymptotic responses of periodicity M occur. Each subregion R_M^J can be characterized by a response ma-

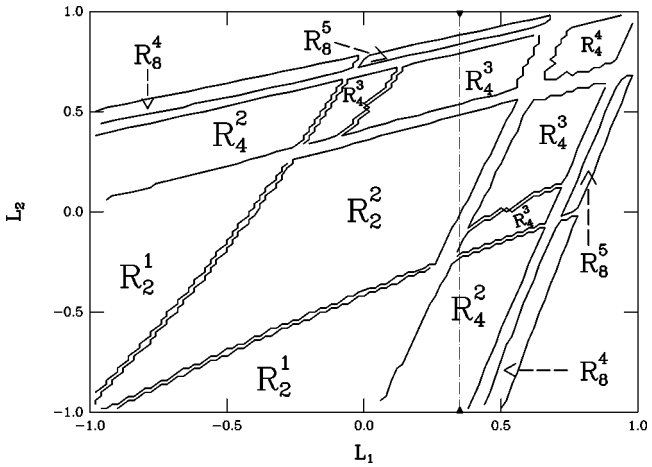

FIG. 1. Main subregions R_M^J for the driven logistic map with $P=2$. Parameter values are $r=1.7$ and $\epsilon=0.2$. The line at $L_1=0.35$ is shown as a guide for Fig. 2.

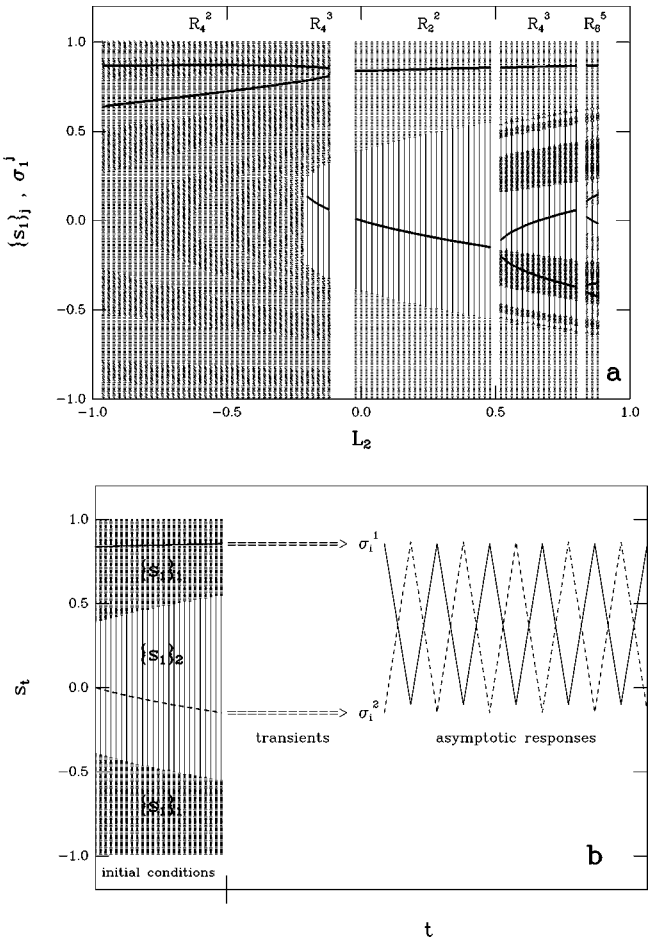

FIG. 2. (a) σ_1^j (thick curves) as functions of L_2 with fixed $L_1=0.35$; the various sets of initial conditions $\{s_1\}_j$ that lead to different σ_i^j are indicated with varying grey tones. The labels on the top correspond to the subregions R_M^J crossed by the vertical line at $L_1=0.35$ in Fig. 1. (b) On the left, the two sets $\{s_1\}_j$ corresponding to the interval labeled as R_2^2 in (a). On the right, the asymptotic responses σ_i^j in time, for $L_1=0.35$ and $L_2=0.48$.

trix $\boldsymbol{\sigma}(\vec{L})$ of size $J\times M$. In particular, the subregion R_P^J is relevant, since there the asymptotic responses of the driven map have the same periodicity than the drive, and consequently the analogy between Eqs. (1) and (2) can be established.

As an illustration, Fig. 1 shows the main subregions R_M^J resulting from Eq. (2) for a logistic map $f(x)=1-rx^2$, driven by different L_t with the same period $P=2$. Parameter values are $r=1.7$ and $\epsilon=0.2$. The subregions R_M^J indicate where J asymptotic responses of maximum periodicity M occur when the components L_1 and L_2 of $\vec{L}$ lie on the range $[-1,1]$. As expected, this diagram is symmetric about the diagonal $L_1=L_2$. The subregion R_4^3 consists of three different asymptotic responses having periods 2, 4, and 4. The five different asymptotic responses in subregion R_8^5 have periods 2, 8, 8, 8, and 8. Each of the other indicated subregions R_M^J consist of J different asymptotic responses having the same period M. The structure of this diagram is actually more complex; there are small zones in between the marked subregions where the driven map reaches a variety of periodic responses (not shown in Fig. 1). We have also observed shrimplike structures for L_1 and L_2 outside the range $[-1,1]$, similar to those reported for two-parameter maps [15].

Figure 2(a) shows, for the same parameters used in Fig. 1, the dependence of the asymptotic responses σ_1^j on both the initial condition s_1 and the component L_2 for a periodic drive with $P=2$. The value of L_1 is fixed to 0.35. As it can be seen in Fig. 1, the subregions R_4^2, R_4^3, R_2^2, R_4^3, and R_8^5 are found when increasing L_2 with fixed $L_1=0.35$. For each value of L_2, Fig. 2(a) indicates with varying gray tones, the various sets of initial conditions $\{s_1\}_j$ that lead to different asymptotic responses σ_i^j. The thick curves in Fig. 2(a) correspond to the J values adopted by the first row of the matrix $\boldsymbol{\sigma}$, i.e., σ_1^j, as functions of L_2. Figure 2(b) shows, on the left, the two sets of initial conditions $\{s_1\}_j$ in the subregion R_2^2 of Fig. 2(a) for $L_2\in[-0.02, 0.48]$ and $L_1=0.35$. On the right, Fig. 2(b) shows the two asymptotic responses σ_i^j in time, for $L_1=0.35$ and $L_2=0.48$.

The analogy between a GCM with a given coupling function H_t and an associated driven map can be carried further by defining an associated coupling vector $\vec{\Theta}=(\Theta_1,\ldots,\Theta_i,\ldots,\Theta_P)$, whose components are given by

$$\Theta_i = H(\underbrace{\sigma_i^1,\ldots,\sigma_i^1}_{N_1\text{ times}},\ldots,\underbrace{\sigma_i^k,\ldots,\sigma_i^k}_{N_j\text{ times}},\ldots,\underbrace{\sigma_i^K,\ldots,\sigma_i^K}_{N_J\text{ times}}) \tag{6}$$

The vector $\vec{\Theta}$ depends on the functional form of the global coupling, on the partition in the J asymptotic responses, and on $\boldsymbol{\sigma}$, which itself is function of $\vec{L}$.

Thus the asymptotic behavior of the GCM has been characterized by the matrix $\boldsymbol{\chi}$ and by the vector $\vec{\Phi}$. Similarly, the matrix $\boldsymbol{\sigma}$ and the vector $\vec{\Theta}$ characterize the asymptotic behavior of the associated driven map. The main point is that an equivalence between both systems arises when $M=P$ and $J=K$, and simultaneously the condition $\vec{\Theta}=\vec{L}$ is fulfilled. If $\vec{L_*}$ is a solution of this set of P nonlinear equations, then the self-consistent response matrix $\boldsymbol{\sigma}(\vec{L_*})$ will also describe an OCB for which $\vec{\Phi}=\vec{L_*}$. In other words, if $\vec{\Phi}=\vec{\Theta}=\vec{L_*}$, a set of N independent driven maps consisting at time i of N_1 maps with the value σ_i^1, N_2 maps with $\sigma_i^2,\ldots,$ and N_K maps with σ_i^K, is undistinguishable from a GCM displaying an OCB characterized by $\boldsymbol{\chi}=\boldsymbol{\sigma}(\vec{L_*})$, and a distribution of elements in clusters given by $N_1,\ldots,N_k,\ldots,N_K$. Obviously, this OCB is a period P solution of Eq. (1). This equivalence is the basis for the method presented in the next section.

III. METHOD FOR PREDICTING CLUSTERED OCB IN GLOBALLY COUPLED MAPS

Now suppose that we want to find out, for a given GCM system described by Eq. (1), if an OCB with the following characteristics can be observed: (i) collective period P, and (ii) a distribution of elements in K clusters corresponding to a partition $\{p_k\}=\{p_1,p_2,\ldots,p_K\}$, where $p_k=N_k/N$ is the fraction of elements in the kth cluster. Then, based on the analogies presented in Sec. II, the following procedure may be employed to answer this question:

(a) Determine if there exists a region R_P^K in which the response matrix $\boldsymbol{\sigma}$ is $K\times P$, by exploring the asymptotic responses of the associated driven map [Eq. (2)], for different drives L_t of the same period P.

(b) Construct the associated coupling vector $\vec{\Theta}=(\Theta_1,\ldots,\Theta_i,\ldots,\Theta_P)$, whose components are given by Eq. (6), by taking $N_k=p_k\,N$.

(c) In the region R_P^K of the P-dimensional $\vec{L}$ space, construct the vector field

$$\vec{V}=\vec{L}-\vec{\Theta}. \tag{7}$$

If the resulting vector field $\vec{V}$ in the region R_P^K is such that (1) it has a locus where $\vec{V}=0$, and (2) it is convergent toward this locus, then an OCB having characteristics (i) and (ii) can, in general, take place for appropriate initial conditions in the GCM system.

As argued in Sec. II, condition (1) implies the existence of an OCB solution for Eq. (1), characterized by $\boldsymbol{\chi}=\boldsymbol{\sigma}(\vec{L_*})$, with the partition $\{p_1,p_2,\ldots,p_K\}$. That is, this method provides a graphic approach for finding a solution $\vec{L_*}$ to the set of the P nonlinear equations $\Theta_i=L_i$.

Condition (2) is related to the evolutive tendency of the GCM toward this OCB solution. At each point $(L_1,\ldots,L_P)$ on the R_P^K region, a vector $\vec{V}$ can be drawn with its origin at this point and its tip at the point $(\Theta_1,\ldots,\Theta_P)$, which is simply the succession of the P values adopted by the coupling function H when evaluated at the asymptotic states contained in $\boldsymbol{\sigma}(L_1,\ldots,L_P)$. Then, because of the analogies between a GCM system and its associated driven map, it is expected that the global coupling H_t of a GCM having a sequence of values matching the set $(L_1,\ldots,L_P)$ will tend to evolve in the direction of the vector $\vec{V}$ located at $(L_1,\ldots,L_P)$. It is also expected that the ability of the vector $\vec{V}$ to signal the evolutive tendency of a GCM increases as the

transient states of the GCM become similar to the states contained in matrix $\boldsymbol{\sigma}(L_1, \ldots, L_P)$. If the vector field $\vec{V}$ is convergent toward a locus where $\vec{V}=0$, then a GCM falling in this convergent region should evolve toward the state described by $\boldsymbol{\sigma}(\vec{L_*})$. The set of partitions $\{p_k\}$ for which the vector field $\vec{V}$ satisfies conditions (1) and (2) are those that can arise in the GCM system for appropriate initial conditions. The method does not tell which initial conditions of the GCM will be conducive toward a specific partition in this set of possible $\{p_k\}$.

There exist some cases in which the coupling H_t does not reach the solution $\vec{V}=0$ but remains around it, even when the field $\vec{V}$ is convergent. As shown in one of the applications below, the OCB in these cases may still be clustered but quasiperiodic. A detailed study of the properties that the field $\vec{V}$ must possess in order to be associated with quasiperiodic OCB's is out of the scope of this paper.

The form of the vector field $\vec{V}$, and that of the locus $\vec{V}=0$, depend on both the local map and the coupling function. The emergence of an OCB in a GCM is the result of the interplay between local dynamics and the global coupling, both being integral parts of the system. In fact, the method allows one to explore the effect of varying either ingredient of the GCM [Eq. (1)], through the changes in the geometry of the vector field $\vec{V}$, which is obtained from the asymptotic response of the associated driven map [Eq. (2)].

The method can be applied whenever the associated periodically driven map exhibits periodic asymptotic behaviors in some regions of the $\vec{L}$ space. There is a large family of maps which satisfy this condition. Notice that the method does not require a previous knowledge of the occurrence of the searched OCB in a given GCM to predict its existence. Additionally, the method provides at least one initial condition $\{x_1^n\}=\{x_1^1, x_1^2, \ldots, x_1^N\}$ to put the associated GCM in the predicted OCB: it suffices to take, as the initial condition $\{x_1^n\}$ of the GCM, the initial condition prescribed by any row of the matrix $\sigma(\vec{L_*})$. Many other initial conditions $\{x_1^n\}$ may evolve toward this particular OCB; however, the method does not give this information.

The partition $\{p_k\}$ can be varied to predict all possible OCB's by looking at the convergence of the vector field $\vec{V}$ and at the locus $\vec{V}=0$ as a function of $\{p_k\}$. Moreover, the first step of the procedure (and the most time consuming) must be executed only once for a given local dynamics f and coupling strength ϵ; thereafter, steps (b) and (c) can be performed repeatedly for many different functional forms of the coupling H and different partitions $\{p_1, p_2, \ldots, p_K\}$. In this way, one can efficiently explore the possible occurrence of various types of OCB's in different GCM systems with the same local dynamics, but different coupling functions.

As mentioned, the vector field $\vec{V}$ is related to the transient trajectory of the GCM. In order to visualize this relation, one can perform direct simulations on the GCM and overlap the dynamics of the global coupling H_t on the associated vector field $\vec{V}$. As it will be seen in the applications, the vector field $\vec{V}$ acts as an indicator of the transient trajectory of the coupling function H_t toward its asymptotic periodic behavior $\vec{\Phi}=\vec{L_*}$. During this transient interval, the elements of the system segregate in ''swarms'' which progressively shrink, and eventually form clusters. Simultaneously, H_t evolves toward its asymptotic behavior. For an initial condition $\{x_1^n\}$ that leads to the partition $\{p_k\}$, the trajectory of H_t toward $\vec{\Phi}=\vec{L_*}$ can be represented in the P-dimensional $\vec{L}$ space as a trajectory joining the point $(H_1, \ldots, H_P)$ to $(H_{P+1}, \ldots, H_{2P})$ to $(H_{2P+1}, \ldots, H_{3P})$, ..., to $(\Phi_1, \ldots, \Phi_P)=\vec{\Phi}$. The transient trajectory of H_t can be superposed to the vector field $\vec{V}$ corresponding to the partition $\{p_k\}$. Then the geometry of $\vec{V}$ and the transient trajectory of the coupling function H_t toward its asymptotic periodic behavior $\vec{\Phi}=\vec{L_*}$ can be compared. This is a way to test the ability of $\vec{V}$ as indicator of the transient trajectory of H_t.

It should be noted that, without a direct simulation on the GCM system, steps (a)–(c) of the method can be performed, and conditions (1) and (2) can be checked, in order to predict that there must exist initial conditions $\{x_1^n\}$ that conduce the GCM toward the locus $\vec{V}=0$.

IV. APPLICATIONS

In order to show applications of the procedure, we choose globally coupled logistic maps $f(x)=1-rx^2$ in their chaotic range, and look for an OCB consisting of two clusters of period 2. Different coupling functions will be considered. Parameter values are fixed at $r=1.7$ and $\epsilon=0.2$ in the first three examples that follow. In the last example, $r=2$, and ϵ is varied.

(1) As a first example, the coupling function H_t is assumed to be the arithmetic mean, i.e., $H_t=(1/N)\Sigma_{n=1}^{N} x_t^n = \langle x \rangle_t$. Therefore, $\Theta_i=p_1\sigma_i^1+p_2\sigma_i^2$, and $V_i=\Theta_i-L_i$, $(i=1,2)$. Figure 3(a) shows the vector field $\vec{V}(L_1,L_2,p_1)$ in the region R_2^2 for partitions $p_1=0.56$ and $p_2=1-p_1$. The vector field $\vec{V}(L_1,L_2,p_1)$ is plotted as arrows of length proportional to $|\vec{V}|$, its direction given by $\tan^{-1}(V_1/V_2)$, and its origin at (L_1,L_2). For different partitions the vector field $\vec{V}$ maintains the same appearance, except that the point where $\vec{V}=0$ moves along the dashed curve in Fig. 3(a) as p_1 varies. The dashed curve is the locus $\vec{V}=0$ as a function of p_1. The two labeled values of p_1 at the ends of the dashed curve in Fig. 3(a) indicate the position of the convergent point $\vec{V}=0$ for these critical values of p_1. The marks on this curve are made at intervals of 0.02 in p_1. Thus the method predicts that an OCB of period 2 with two clusters can be observed in the GCM, and that the possible values of p_1 will lie in the range $[0.38,0.62]$. However, as stated above, the method does not provide the initial condition $\{x_1^n\}$ of the GCM that will lead to a specific value of p_1.

In order to make a direct comparison between both, the field $\vec{V}$ and the transient dynamics of H_t obtained from direct simulation of the GCM system, Fig. 3(b) shows their superposition. The dynamics of H_t corresponds to a GCM with $N=2000$ elements starting from initial conditions distributed on $[-1,1]$ with uniform probability, i.e., $\langle x \rangle_1=0$. In this case, direct simulation shows that the GCM rapidly collapses into two clusters with the partition $N_1=954$ and $N_2=1046$,

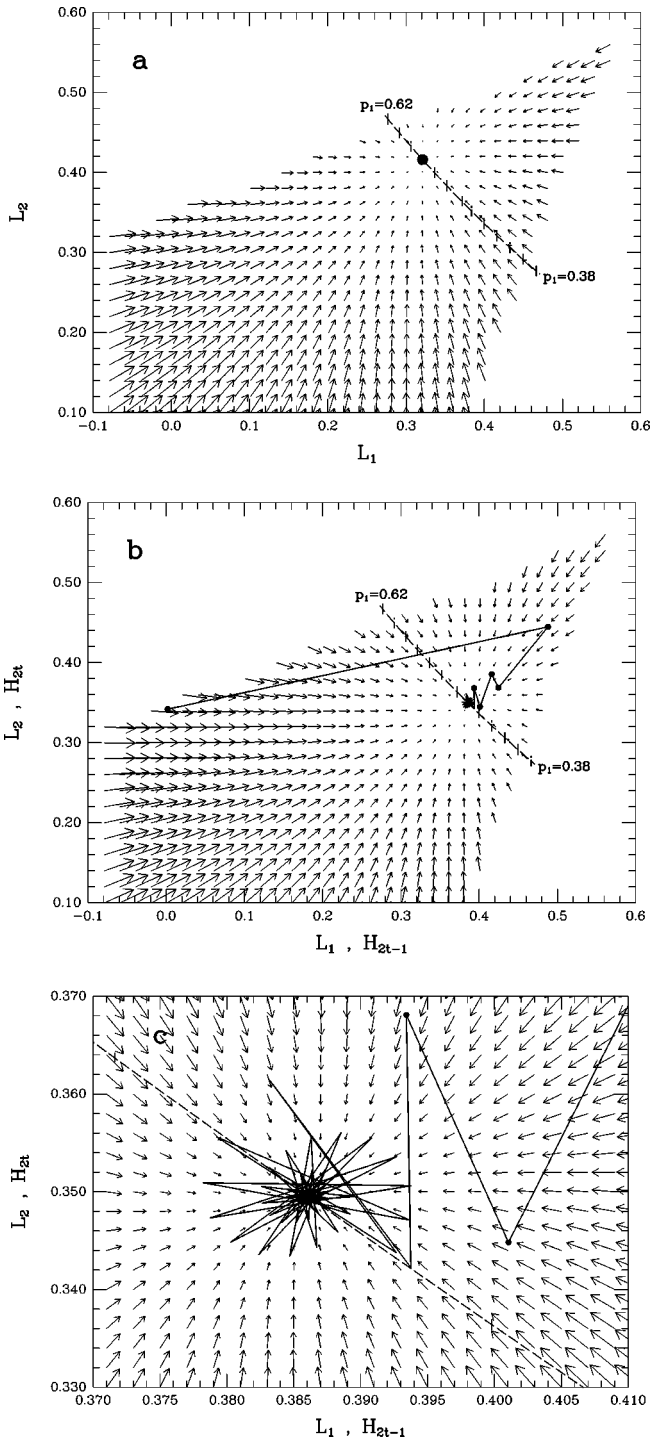

FIG. 3. (a) The vector field $\vec{V}$ in the region R_2^2 for an arithmetic mean coupling function and a partition $p_1=0.56$. The dashed curve is the locus $\vec{V}=0$ as a function of p_1. (b) Comparison of the vector field $\vec{V}$ and the trajectory of H_t for a particular case. (c) Magnification of (b). See example (1).

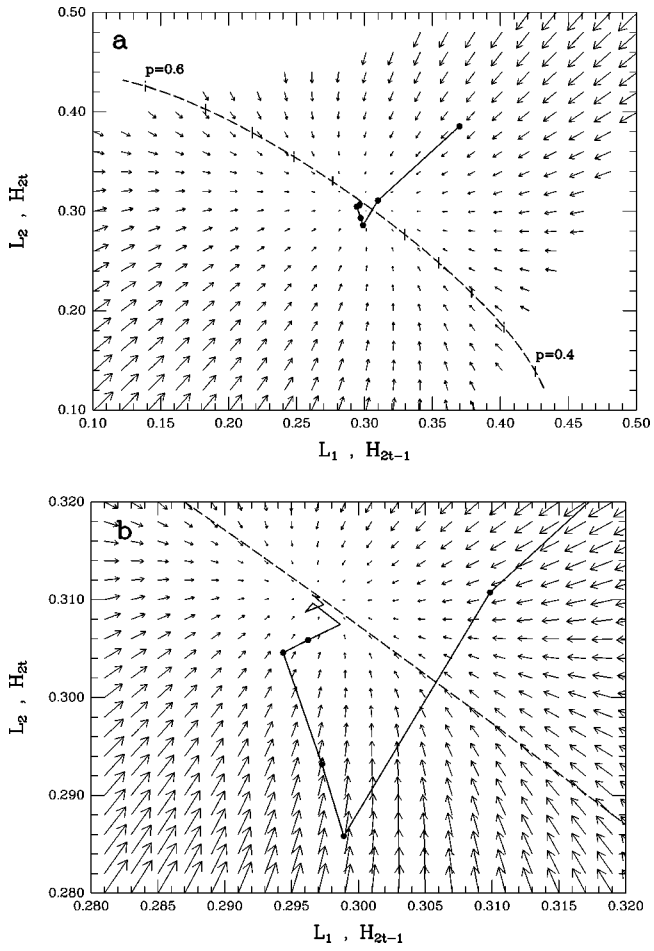

FIG. 4. (a) Comparison of the vector field $\vec{V}$ and the trajectory of H_t for the geometric mean coupling. (b) Magnification of (a). See example (2).

i.e., $p_1=0.477$. The trajectory of the coupling function H_t is represented in Fig. 3(b) by joining (H_1,H_2) to (H_3,H_4), . . . , to (Φ_1,Φ_2). The vector field $\vec{V}(L_1,L_2,p_1)$ in the region R_2^2 is shown for the same partition $p_1=0.477$. Note that, for the first few iterations, the H_t transient trajectory is roughly suggested by the field $\vec{V}$, since at these early stages the cluster are being formed. As time progresses, the vector field $\vec{V}$ becomes a better indicator of the evolution of the GCM system toward its OCB, as shown in Fig. 3(c). As it can be seen in Figs. 3(b) and 3(c), the vector field $\vec{V}$ contains valuable information on how a GCM system converges toward an OCB. The comparison presented in Figs. 3(b) and 3(c) has been used to verify this property of the vector field $\vec{V}$ in a particular case. However, it should be emphasized that this verification is not required in order to apply the proposed method to predict the existence of OCB's.

(2) In a second example, we consider the geometric mean of the moduli of the values of the elements of the system as the coupling function, i.e., $H_t=\Pi_{n=1}^{N}|x_t^n|^{1/N}$. Therefore, in the region R_2^2, $\Theta_i=|\sigma_i^1|^{p_1}\times|\sigma_i^2|^{1-p_1}$ $(i=1,2)$. Figure 4(a) shows the comparison of the vector field $\vec{V}$ corresponding to $p_1=0.505$ and the trajectory of the coupling function H_t. The same initial conditions and system size as in the first example have been used. The dashed curve is the locus $\vec{V}=0$ as a function of p_1. In this case, the convergence to the OCB is faster than that observed in the first example, as shown in Fig. 4(b).

(3) Even when the associated driven map has periodic asymptotic regimes in the region R_P^K, the collective behavior of the corresponding GCM [Eq. (1)] is not always periodic. In those cases the matrix $\boldsymbol{\chi}$ can not be constructed, but the

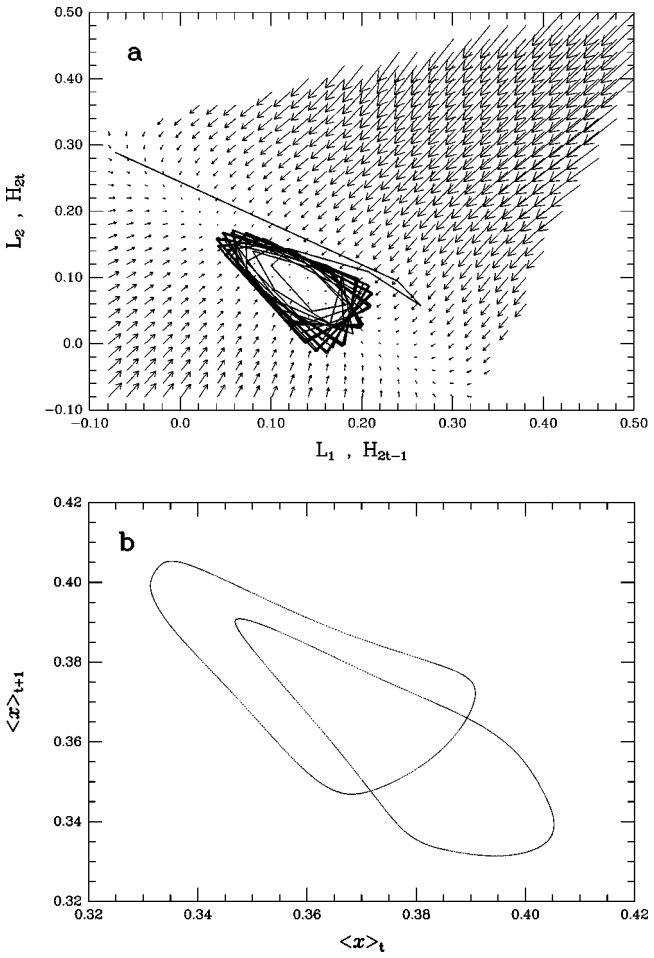

FIG. 5. (a) The vector field $\vec{V}$ and the trajectory of H_t for the modified arithmetic mean global coupling. (b) The asymptotic return map of the mean state of the system. See example (3).

vector field $\vec{V}$ is still useful. In this example, the method will be used to infer a global coupling function capable of producing a quasiperiodic OCB with two clusters. This can be achieved by modifying the coupling function of a known case of periodic OCB, just near its convergent point $\vec{V}=0$. Then we may expect that the modified GCM will not reach its original periodic OCB, but would remain close to it. For the first example, this can be done by noticing that when $\vec{L}$ is near the convergent point, one of the two asymptotic responses of the driven map in R_2^2 adopts a value close to 0.86 every two time steps (i.e., σ_1^1 in Fig. 2). Then the coupling function of the first example may be modified in such a way that only near 0.86 the function is drastically affected. We have tried with coupling functions of the type:

$$H_t=\frac{1}{N}\sum_{n=1}^{N} x_t^n\left\{1-a\left[1-\exp\left(\frac{1}{b(x_t^n-0.86)^2}\right)\right]\right\}. \quad (8)$$

The resulting vector field $\vec{V}$ and the transient trajectory of H_t for parameters values $a=1.7$ and $b=-10^3$ in Eq. (8) are shown in Fig. 5(a). Additionally, the asymptotic behavior of the return map of the mean field of the GCM is shown in Fig. 5(b). This example shows the usefulness of the method for designing globally coupled systems with specific features.

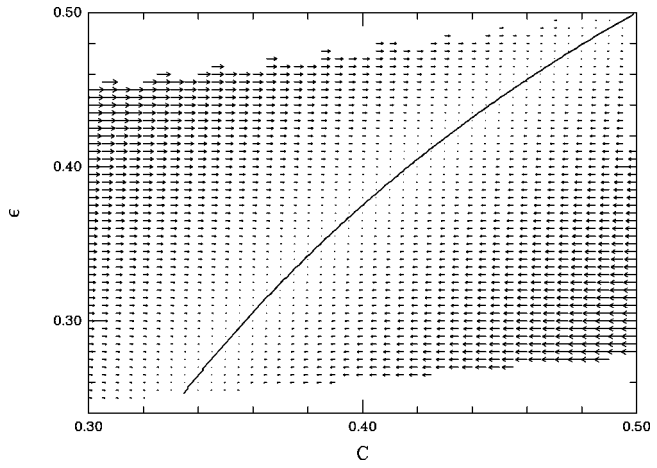

FIG. 6. The vector field $\vec{V}$ for two identical out of phase clusters of period 2, on the plane (C,ϵ). The continuous curve corresponds to the locus $\vec{V}=0$. See example (4).

The geometry of the locus $\vec{V}=0$ and the type of convergence toward it are related to different kinds of collective states, such as periodic or quasiperiodic OCB's. A quasiperiodic OCB appears to be associated with a type of convergence of the field $\vec{V}$ occurring in this example. This type of convergence may also occur for other functional forms of f and H.

(4) As a last example, for an arithmetic mean global coupling $H_t=\langle x\rangle_t$, the method will be used to find OCB's consisting of two identical out of phase clusters of period 2 (i.e., $p_1=p_2=0.5$) that result in a constant $H_t=C$. In this case, it is sufficient to calculate the response matrix $\boldsymbol{\sigma}$ in the region R_2^2 for drives $L_1=L_2=C$. The vector field $\vec{V}$ lies on the line $L_1=L_2$ because $\Theta_1=\frac{1}{2}(\sigma_1^1+\sigma_1^2)=\Theta_2=\frac{1}{2}(\sigma_2^1+\sigma_2^2)$, i.e., the two asymptotic responses are out of phase, and their sum is constant in time. In the present example, the field $\vec{V}=(\Theta_1-C,\Theta_2-C)$ can be represented on the plane (C,ϵ) as horizontal arrows of length proportional to $|\vec{V}|$, direction given by the sign of Θ_1-C, and origin at C. Taking advantage of its unidirectionality, the vector field $\vec{V}$ is plotted in Fig. 6 on the plane (C,ϵ), for the logistic map at $r=2.0$. The continuous curve corresponds to the locus $\vec{V}=0$. In this example, the method has been used for $K=2$ and $P=2$, but it may also be applied to predict OCB's with other numbers of K identical out of phase clusters with periodicity P resulting in a constant mean field in other ranges of ϵ.

V. CONCLUSIONS

We have presented a method to study the emergence of ordered collective behaviors in globally coupled maps, based on the analogy between these systems and a driven map. A vector field defined on the space of the drive term in the driven map acts as an indicator of the evolution of the coupling function in the GCM. The field $\vec{V}$ is particularly efficient in pointing the transient trajectory of the coupling function when the associated driven map reaches its asymptotic periodic response in few iterations. The method can be used to predict if specific types of OCB's can take place in a GCM system, and to visualize its associated basin of attraction. In

the examples with mean field coupling, several clustered OCB's were predicted to occur in globally coupled logistic maps, in accordance to numerical simulations performed by Kaneko [10]. Examples (3) and (4) have illustrated how to use the procedure for other functional forms of the global coupling. It is interesting to note that quasiperiodic OCB's may occur in regions where the associated driven map has periodic asymptotic regimes, as shown in example (3). A detailed study of the necessary properties that the vector field $\vec{V}$ must possess in order to be associated to a periodic or quasiperiodic OCB would be an interesting problem for future work. In the examples, the field $\vec{V}$ could be represented on a plane, but, for $P \geqslant 3$, projections of $\vec{V}$ may serve to reveal its global structure. As P increases, the computation time increases potentially with P. Then numerical methods to search for convergence toward $\vec{V}=0$ may be used to speed up the process.

The limitation of this method lies on the fact that the associated driven map must possess periodic asymptotic responses, so that the matrix $\boldsymbol{\sigma}$ may be defined. A large family of maps fulfills this condition. The examples presented here show that progress in the understanding of the collective behaviors of the GCM can be made by investigating its relation with driven maps. Recently, this relation was noticed in Ref. [16]. Extensions of the method presented here could be applied to other phenomena in globally coupled systems, such as control of chaos, chaotic synchronization, phase segregations, and intermittent OCB's.

ACKNOWLEDGMENTS

This work was supported by Consejo de Desarrollo Científico, Humanístico y Tecnológico, of the Universidad de Los Andes, Mérida, Venezuela.

[1] See *Theory and Applications of Coupled Map Lattices*, edited by K. Kaneko (Wiley, New York, 1993); Chaos **2** (3) (1992), focus issue on CML, edited by K. Kaneko.
[2] K. Kaneko, Phys. Rev. Lett. **65**, 1391 (1990).
[3] N. Chatterjee and N. Gupte, Phys. Rev. E **53**, 4457 (1996).
[4] H. Chaté, A. Lemaitre, P. Marq, and P. Manneville, Physica A **224**, 447 (1996).
[5] H. Chaté and P. Manneville, Europhys. Lett. **17**, 291 (1992); Prog. Theor. Phys. **87**, 1 (1992).
[6] K. Wiesenfeld, C. Bracikowski, G. James, and R. Roy, Phys. Rev. Lett. **65**, 1749 (1990).
[7] S. H. Strogatz, C. M. Marcus, R. M. Westervelt, and R. E. Mirollo, Physica D **36**, 23 (1989).
[8] N. Nakagawa and Y. Kuramoto, Physica D **75**, 74 (1994).
[9] K. Kaneko, Physica D **75**, 55 (1994); **77**, 456 (1994).
[10] K. Kaneko, Physica D **41**, 137 (1990).
[11] K. Kaneko, Physica D **86**, 158 (1995).
[12] G. Perez, S. Sinha and H. A. Cerdeira, Physica D **63**, 341 (1993).
[13] K. Kaneko, Physica D **54**, 5 (1991).
[14] A. Pikovsky and J. Kurths, Physica D **76**, 411 (1994).
[15] J. A. C. Gallas, Physica A **202**, 196 (1994).
[16] T. Chawanya and S. Morita, Physica D **116**, 44 (1998).